

## SUPPORTING ONLINE MATERIAL for J. Burré et al.,

### “ $\alpha$ -Synuclein Promotes SNARE-Complex Assembly in vivo and in vitro”

#### MATERIALS & METHODS

##### Abbreviations

Ab	Antibody
AP5	Amino-Phosphonopentanoate
BoNT/B	Botulinum toxin B light chain
Casp-3 <sup>CL</sup>	Cleaved caspase-3
CNQX	6- Cyano-7-nitroquinoxaline-2,3-dione
Cpx	Complexin
CSP $\alpha$	Cysteine string protein-alpha
CSP <sup>-/-</sup>	CSP $\alpha$ KO
DIV	Days in vitro
GDI	Guanine nucleotide dissociation inhibitor
GFAP	Glial fibrillary acidic protein
fEPSP	field excitatory postsynaptic potential
Hsc70	Heat shock cognate protein of 70 kDa
KO	Knockout
LAMP-2	Lysosome-associated membrane protein 2
NF-H	Neurofilament heavy chain
NSF	N-ethyl maleimide sensitive factor
OG	n-Octyl- $\beta$ -D-glucoside
PSD-95	Postsynaptic density protein 95
SCAMP-1	Secretory carrier membrane protein 1
SDS	Sodium dodecyl sulfate
SGT	Small glutamine-rich tetratricopeptide repeat-containing
$\alpha$ SNAP	Soluble N-ethylmaleimide sensitive fusion protein-attachment protein
SNAP-23	Synaptosomal-associated protein of 23 kDa
SNAP-25	Synaptosomal-associated protein of 25 kDa
SNARE	Soluble NSF attachment protein receptor
Syb2	Synaptobrevin-2
Synt-1	Syntaxin-1
$\alpha$ -Syn	$\alpha$ -Synuclein
Syp	Synaptophysin
Syt1	Synaptotagmin-1
TeNT	Tetanus toxin light chain
TKO	$\alpha/\beta/\gamma$ -synuclein triple knockout
TTX	Tetrodotoxin
tSyn	Transgenic overexpressed alpha-synuclein
TX-100	Triton X-100
VCP	Valosin-containing protein
vGAT	Vesicular GABA transporter
WT	Wild-type

**Mouse breeding, aging and survival studies.** CSP $\alpha$  KO mice (CSP<sup>-/-</sup>) (S1) were bred as a pure or as a compound line with  $\alpha$ -synuclein transgenic mice as described (S2). CSP $\alpha$  mice rescued by the transgenic expression of human  $\alpha$ -synuclein (tSyn/CSP<sup>-/-</sup>) (S2) were bred as tSyn/CSP<sup>+/-</sup> to CSP<sup>+/-</sup> in order to keep the transgene expression constant.  $\alpha/\beta/\gamma$ -synuclein triple KO (TKO) mice were obtained by crossing the  $\alpha/\beta$ -synuclein double KO mice (S3) with previously generated  $\gamma$ -synuclein

KO mice (*S4*). Less than 4 mice per cage were allowed to age and were monitored at least once a week. As the mice grew weaker, due to progressive neuromuscular impairments, they were monitored daily and were provided with wet food on the floor of the cage. When mice had a level of paralysis which inhibited their access to food or water, they were sacrificed, the date was recorded as the date of death and the brain was harvested for pathological studies. The animal protocols used in this study, as well as the overall mouse and rat husbandry practices were approved by the respective Institutional Animal Care and Use Committees (IACUCs) at Stanford University.

**Behavioral studies in mice.** Mice were analyzed by weight measurements and neurological tests as follows: *Hind limb clasping* (*S5*) was used to assess onset of motor impairment. Mice were suspended from the tail for 1 min to induce limb clasping. Onset is defined as the first day when hind limb clasping was observed. For the *Grid hanging* test (*S6*), animals were placed on top of a wire mesh grid. The grid is then shaken lightly 3 times to cause the mouse to grip the wires and turned upside down. The mesh was held approximately 20 cm above the home cage litter, high enough to prevent the mouse of easily climbing down but not to cause harm in the event of a fall. A stopwatch was used to record the time taken by the animal to fall off the grid. Three trials per mouse were performed with a 1 min inter-trial interval. The mean of the 3 trials was assigned as the latency of each animal to fall. *Grip strength* test (*S7*) (using a grip strength meter; Columbus Instruments) was used to measure grasping strength in the paws. The grip strength meter was positioned horizontally, and mice were held by the tail and allowed to grasp the metal mesh pull-bar either with four limbs or with the forelimbs only. The animals were then pulled back and the force applied to the bar at the moment the grasp was released was recorded. Mice were given 3 trials using all four limbs and 3 additional trials using the forelimbs with 1 min inter-trial intervals. The mean of the 3 trials was assigned for the grip strength of each animal. *Rotarod* test (*S8, S9*) (using an Accelerating Rotarod; Med Associates Inc.) was used to assess motor coordination and motor learning. Mice were placed on the Rotarod which slowly accelerated from 3 to 30 rounds per minute over 5 minutes. Mice were given 3 trials per day for 3 days with 30-40 min inter-trial intervals. Time to fall from the rotarod (latency) was recorded for each trial. Mice that remained on the Rotarod for the whole 5 min trial were assigned a 300 second latency. *Beam walking* test (*S9*) was used to record deficits in balance and limb control (accuracy and strength in limb placement). Animal's ability to navigate across a beam to return to its home cage was tested using a wooden dowel (cylindrical beam 60 cm in length, 1 cm in diameter). The beam was steadily fixed on both ends 40 cm above the ground leading to a small cage filled with bedding from the animal's home cage. Mice were placed onto one side of the beam and were left to cross the beam to reach the cage. Mice that escaped into the cage were picked up and placed on the opposite side again for a total of 3 trials with 1 min inter-trial intervals. Sessions were videotaped and the number of footslips for each mouse per trial was scored.

**Primary cultures of rat and mouse neurons.** Rat hippocampal or mouse cortical neurons were cultured from newborn rats or mice essentially as described (*S10, S11*). Brain regions were dissected in ice-cold Hank's Balanced Salt Solution (HBSS), dissociated by trypsinization (0.05% trypsin-EDTA, for 10 min at 37 °C), triturated with a siliconized pipette, and plated (100  $\mu$ l) onto a 12 mm coverslip (for immunofluorescence) or on 12-well plastic dishes, coated for at least 30 min with Matrigel (BD Biosciences). Plating medium (MEM (Gibco) supplemented with 5 g/l glucose, 0.2 g/l NaHCO<sub>3</sub> (Sigma), 0.1 g/l transferrin (Calbiochem), 0.25 g/l insulin (Sigma), 0.3 g/l L-glutamine (Gibco), and 10% fetal bovine serum) was replaced with growth medium (MEM (Gibco) containing 5 g/l glucose, 0.2 g/l NaHCO<sub>3</sub> (Sigma), 0.1 g/l transferrin (Calbiochem), 0.3 g/l L-glutamine (Gibco), 5% fetal bovine serum, 2% B-27 supplement (Gibco), and 2  $\mu$ M cytosine

arabinoside (Sigma) 24-48 h after plating. Neuronal cultures were transduced with recombinant lentiviruses and/or used for experiments as indicated.

**Lentiviral vector production, transduction and expression of  $\alpha$ -Synuclein.** A c-Myc epitope with a 4 amino acid linker was introduced into FUW lentiviral vector at the N-terminus of human  $\alpha$ -synuclein with deletion of the original methionine of  $\alpha$ -synuclein, resulting in the following N-terminal sequence: MEQKLISEEDLGSGS. For the  $\alpha$ -synuclein truncation construct, a stop codon was introduced at residue 96. FUW vector (containing  $\alpha$ -synuclein variants), VSVG envelope glycoprotein and  $\Delta$ 8.9 HIV-1 packaging vectors were co-transfected (in a 1:1:1 molar ratio) into HEK293T cells (ATCC) using Fugene-6 (Roche) (*S11-S13*). Medium was changed to neuronal growth medium after 8-12 h. Medium containing the viral particles was collected 48 h later and centrifuged for 10 min at 2,000 rpm to remove any cellular residues. The supernatant containing the virions was added to cultured neurons at 2-7 days in vitro (DIV), and the expression of the recombinant proteins was monitored using GFP fluorescence for at least 7 days post infection (DPI) before the beginning of the experiment.

**Immunocytochemistry.** Performed essentially as described (*S14*), cultured neurons infected with lentiviruses encoding myc-tagged  $\alpha$ -synuclein were washed 3 times with PBS, and fixed for 20 min at room temperature in PBS containing 4% paraformaldehyde. Following three washes with PBS, the fixed cultures were permeabilized for 15 min in blocking solution (PBS containing 5% BSA (Sigma)) supplemented with 0.1% Triton X-100 (Sigma). Cultures were incubated with c-myc antibody (Santa Cruz, monoclonal, 1:200 in blocking solution) overnight at 4 °C, followed by anti-mouse Alexa 488 secondary antibody (1:500) for 1 h in blocking solution. Synapsin antibodies (E028, polyclonal, 1:1000) were used as a synaptic marker, followed by anti-rabbit Alexa 633 secondary antibody (1:500), both incubated for 1 h each in blocking solution. The coverslips were rinsed six times with PBS, mounted on slides in Vectashield aqueous mounting medium (Vector Labs) and stored at 4 °C. Laser scanning confocal microscopy was performed to compare localization, with serial excitation at 633 nm and 488 nm, on a Leica TCS SP-2 inverted microscope. For analysis of synaptic targeting of  $\alpha$ -synuclein, individual channels for  $\alpha$ -synuclein and synapsin were compared for co-localization using ImageJ (Pearson's coefficient).

**Immunohistochemistry.** Anesthetized mice were perfused with ice-cold 4% paraformaldehyde in PBS, followed by removal of the brain and overnight fixation in 4% paraformaldehyde in PBS (room temperature). Fixed brains were cryopreserved in 30% sucrose in PBS for 2 days and frozen in Tissue Tek OCT embedding medium (Sakura Finetechnical). Sagittal brain sections (20  $\mu$ m) were cut at -20 °C (Leica CM3050S cryostat), picked up on slides and heat-adhered at 37 °C for 30 min. For immunostaining, slides were incubated in blocking solution (3% BSA, 0.1% Triton X-100 in PBS) for 1 h followed by overnight incubation with primary antibodies (4 °C). Slides were washed 3 times in PBS (5 min each) and incubated in blocking buffer containing Alexa Fluor 488- or Alexa Fluor 633-coupled secondary antibodies (Molecular Probes) for 3 h at room temperature. Following 6 washes in PBS, slides were mounted with Vectashield hard-set mounting medium with DAPI (Vector) followed by fluorescence microscopy. Puncta of NeuN and DAPI in the images were counted using ImageJ software (NIH), and the frequency distribution analysis was performed using Prism software (GraphPad).

**Silencing or enhancing synaptic activity.** Similar to previously described methods (*S15, S16*), synaptic activity was pharmacologically manipulated in WT or TKO mouse cortical cultures at DIV10. Synaptic activity was silenced by either inhibiting action potentials with 0.5  $\mu$ M tetrodotoxin (TTX; Calbiochem). Conversely, synaptic activity was enhanced by addition of  $\text{CaCl}_2$  to 4 mM final to the neuronal growth medium. Cells were washed in ice-cold PBS, and immediately

dissolved in 2x SDS sample buffer. For the time course, cells under TTX or CaCl<sub>2</sub> incubation were harvested at the indicated time points.

**Quantitation of SNARE-complexes as high molecular mass bands.** (S17) Whole brains or cortices were homogenized in ice-cold PBS, and immediately dissolved in 2x SDS sample buffer. The lysates were subjected to SDS-PAGE and immunoblotting with antibodies to SNAP-25 (SMI81), and polyclonal antibodies to synaptobrevin-2 (P939) and syntaxin-1 (438B). To measure total SNARE protein levels, samples were boiled for 20 min. SDS-resistant SNARE-complexes were defined as the immunoreactive material above 40 kDa that was absent from boiled samples. Note that as with all other quantitative immunoblotting experiments, <sup>125</sup>I-labeled secondary antibodies were used and signals were measured by phosphorimager scanning.

**Overexpression studies in transfected 293 cells.** For  $\alpha$ -synuclein titration experiments, HEK293T cells were co-transfected with pCMV5-syntaxin-1A, -Syb2, -SNAP-25A (1:1:1), and an increasing amount of a plasmid encoding human  $\alpha$ -synuclein ( $\alpha$ -Syn). Total DNA was kept constant by balancing  $\alpha$ -Syn plasmid with pCMV5-emerald, which expresses a similar sized GFP-derived protein. For studies using tetanus toxin (TeNT) or botulinum toxin B (BoNT/B) light chains, HEK cells were transfected with one of the toxins, and lysates were mixed over night at 4 °C with lysates from HEK cells transfected with Syb2  $\pm$   $\alpha$ -Syn, or SNAREs  $\pm$   $\alpha$ -Syn. For  $\alpha$ -Syn interaction studies, HEK293T cells were co-transfected with either  $\alpha$ -Syn and  $\alpha$ SNAP, or  $\alpha$ -Syn and NSF (1:1 ratio). Two days after transfection, cells were harvested by solubilization in 0.1% TX-100 and subjected to immunoprecipitation or immunoblotting.

**Recombinant protein expression and purification.** All proteins were expressed in bacteria (BL21 strain) as GST fusion proteins in modified pGEX-KG vectors (GE Healthcare), essentially as described (S11, S18). *SNAP-25A*, *Syntaxin-1<sup>1-264</sup>*,  *$\alpha$ -synuclein*, *Syb2<sup>1-96</sup>* and  *$\alpha$ SNAP*. Bacteria were grown to OD 0.5 (measured at 600 nm), and protein expression was then induced with 0.01 mM IPTG for 6h at room temperature. Bacteria were harvested by centrifugation for 20 min at 4,000 rpm and 4°C, and pellets were resuspended in solubilization buffer (10 mM Tris-Cl buffer pH 7.4, 150 mM NaCl, 2 mM DTT, 5% glycerol, 0.1% Triton X-100, 0.5 mg/ml lysozyme, 1 mM PMSF and an EDTA-free protease inhibitor cocktail (Roche)). Cells were broken by sonication (3x 15 pulses, 50% output), and insoluble material was removed by centrifugation for 30 min at 7,000 g<sub>av</sub> and 4°C. Proteins were affinity-purified using glutathione sepharose bead (GE Healthcare) incubation overnight at 4°C, followed by thrombin cleavage (10 U per mg protein) overnight at 4°C. *Full length HA-tagged synaptobrevin-2 and HA-tagged syntaxin-1.* Bacteria were grown, induced and harvested as mentioned above. The pellet was resuspended for 20 min at 4°C in solubilization buffer (2% n-octyl- $\beta$ -D-glucoside (OG) in PBS, 0.5 mM EDTA pH 8.0, 0.5 mg/ml lysozyme, 1 mM PMSF, and an EDTA-free protease inhibitor cocktail (Roche), and sonicated (3x 15 pulses, 50% output). Insoluble material was removed by centrifugation as mentioned above. Washed glutathione sepharose beads in 2% OG in PBS were added to the supernatant overnight at 4°C. Beads were washed with 2% OG in PBS, and recombinant protein was cleaved using thrombin. *NSF.* Bacteria were grown to OD 0.8, and protein expression was induced with 0.4 mM IPTG for 5h at room temperature. Bacteria were harvested as described above, and bacterial pellets were solubilized in 100 mM HEPES-KOH pH 7.4 with 500 mM KCl, 2 mM DTT, 1 mM MgCl<sub>2</sub>, 0.5 mM ATP, 10% glycerol, 1 mM PMSF and a protease inhibitor cocktail (Roche, EDTA-free). Bacterial membranes were broken by sonication as mentioned above, and cleared supernatant was added to glutathione sepharose beads in NSF solubilization buffer and incubated overnight at 4 °C. Protein was eluted from the beads using thrombin in solubilization buffer.

**Purified protein-protein interaction studies.** Recombinant GST-fusion proteins (2 µg each) corresponding to either GST- $\alpha$ -Syn WT, GST- $\alpha$ -Syn<sup>1-95</sup> or GST alone on GST-sepharose beads were incubated with 5 µg thrombin-cleaved soluble Syb2<sup>1-96</sup> in 250 µl 0.1% TX-100 in PBS containing protease inhibitors at 4 °C for 2 h. Following 6 washes with 500 µl of ice-cold incubation buffer, proteins were eluted with 2x SDS sample buffer containing 2 mM DTT for 15 min at 37 °C. The eluate was separated by SDS-PAGE for either Coomassie Brilliant Blue staining or for immunoblotting.

**NSF ATPase assay.** 2 µg purified  $\alpha$ SNAP in 20 µl volume were immobilized in a reaction tube for 20 min at RT (S19). To analyze NSF ATPase activity, 1 µg purified NSF with or without addition of 1 µg  $\alpha$ -synuclein ( $\alpha$ -Syn) were added in 50 µl reaction buffer (50 mM HEPES-KOH pH 7.4, 100 mM KCl, 8 mM MgCl<sub>2</sub>, 4 mM ATP) and incubated for 1h at 37°C. Buffer, NSF,  $\alpha$ SNAP and  $\alpha$ -synuclein only incubations were performed as controls. Decreasing ATP levels were assayed at indicated time points using Kinase-Glo reagent (Promega) (S16): 1 µl of the reaction was mixed with 50 µl 50 mM HEPES-KOH pH 7.4 with 100 mM KCl, and 5 µl Kinase-Glo reagent. Samples were incubated for 20 min at RT, and emission was measured at 560 nm using a microplate reader (Mithras LB 940, Berthold Technologies). ATP concentration was determined using an ATP standard curve. Increasing phosphate concentration was assayed according to a modified Lanzetta (S20) protocol: 10 µl sample were incubated for 1 min at RT with 90 µl reaction buffer and 800 µl of Lanzetta solution (preparation: stir three parts 0.045% malachite green with one part 4.2% ammonium molybdate in 4N HCl for 60 min at RT. Add 1 ml 1% TX-100 to 50 ml stirred solution, filter twice, and keep solution in the dark). The reaction was stopped by addition of 100 µl 34% citrate solution. Extinction was measured at 645 nm using a microplate reader (Mithras LB 940, Berthold Technologies). Generated phosphate was determined using a phosphate standard curve.

**Reconstitution of synaptobrevin-2 or syntaxin-1 into liposomes and flotation assay.** Liposome preparation. Liposomes were always prepared on the day of usage, essentially as described (S21). Either 500 µg brain L-alpha-Phosphatidylcholine (PC, Avanti Polar Lipids) or 345 µg PC and 155 µg brain L-alpha-Phosphatidylserine (PS, Avanti Polar Lipids) were mixed with 2.5 µg 1-oleoyl-2-{6-[(7-nitro-2-1,3-benzoxadiazol-4-yl)amino] hexanoyl}-sn-glycero-3-phosphocholine (NBD, Avanti Polar Lipids) in a glass tube. The lipid mixture was dried under a nitrogen stream and for 2h in a speed vac. To form unilamellar, small vesicles, the dried lipids were solubilized in 500 µl 1% n-octyl- $\beta$ -D-glucoside (OG) in 20 mM phosphate buffer pH 7.4, vortexed for 2 min and then sonicated for 3x 15 pulses at 1 sec intervals and 38% sonicator output. Synaptobrevin-2 (Syb2) or syntaxin-1 (Synt-1) reconstitution into liposomes. Performed essentially as described (S22), 100 µl liposomes were mixed with 10 µg HA-synaptobrevin-2 or HA-syntaxin-1 in 2% OG for 1h at RT (ratio of liposomes to protein = 100:1). The protein-lipid-solution was mixed with 300 µl 20 mM phosphate buffer pH 7.4 to dilute OG under its critical micelle concentration to allow incorporation of protein into the PC/PS lipid vesicles. To analyze membrane topology, 0.625 µg liposome-reconstituted protein was incubated with 0.025 µg trypsin for 15 min at RT with or without addition of 0.2% TX-100. To stop proteolysis, 2x SDS sample buffer was added, and samples were analyzed by SDS-PAGE and immunoblotting for HA or by Coomassie brilliant blue staining. Analysis of SNARE-complex formation. Essentially as described (S23), 1 µg SNAP-25 (full length) and 1 µg Synt-1 (residues 1-264) were incubated with 100 µl liposomes with or without reconstituted Syb2 overnight at 4°C in the dark with or without addition of 5 µg  $\alpha$ -synuclein ( $\alpha$ -Syn). Alternatively, plain liposomes were incubated with 5 µg  $\alpha$ -Syn, or 1 µg SNAP-25 (full length) and 5 µg  $\alpha$ -Syn were incubated with 100 µl HA-Synt-1 reconstituted liposomes with or without addition of 1 µg soluble Syb-2 (Syb-2<sup>1-96</sup>). In a centrifugation tube, 100 µl protein samples were mixed with 100 µl 20 mM phosphate buffer pH 7.4 and 200 µl 80% Accudenz reagent (Accurate Chemical &

Scientific corporation) in the same buffer (40% final density), and were carefully overlaid with 200  $\mu$ l 35% and 200  $\mu$ l 30% Accudenz reagent, and 30  $\mu$ l buffer. To achieve separation of bound and non-bound proteins, gradients were centrifuged for 3h at 280,000  $g_{av}$  and 100  $\mu$ l fractions were collected from the top to the bottom of the gradient. The distribution of the liposomes in the gradient was determined by measuring the fluorescence of the lipid derivative NBD in each fraction using a fluorescence plate reader (Mithras LB 940, Berthold Technologies; excitation at 464 nm, emission at 531 nm). For analysis of protein distribution within the gradient, 10  $\mu$ l 5x SDS sample buffer were mixed with 100  $\mu$ l protein sample, and 20  $\mu$ l were separated by SDS-PAGE and immunoblotted for SNARE proteins and  $\alpha$ -synuclein.

**Immunoprecipitations.** Performed essentially as described (*S2*, *S11*), brain, neuronal cultures (DIV15, 11 days post infection) or HEK (2 days post transfection) homogenates were solubilized in phosphate buffered saline (pH 7.4) containing 150 mM NaCl, 1% Triton X-100, supplemented with protease inhibitors at 4 °C. Following centrifugation at 16,000  $g_{av}$  for 10 min at 4 °C, the clarified lysate was subjected to immunoprecipitations with the indicated primary antibodies and 50  $\mu$ l of a 50% slurry of protein-G Sepharose beads (Amersham) for monoclonal IgG, or protein-A sepharose beads (GE healthcare) for polyclonal rabbit sera, for 2 h at 4 °C. Control immunoprecipitations were performed with WT brain lysates with no antibody (for monoclonal antibodies), or with pre-immune serum (for polyclonal rabbit sera). Following 5 washes with 1 ml of the extraction buffer, bound proteins were eluted with 2 x SDS sample buffer containing 10%  $\beta$ -mercaptoethanol and boiled for 15 min at 100 °C. Co-precipitated proteins were separated by SDS-PAGE, with 5-10% of the input in the indicated lane.

**Immunoblotting and protein quantification.** All quantitative immunoblotting experiments were performed with iodinated secondary antibodies as described (*S24*). Samples were separated by SDS-PAGE, and transferred onto nitrocellulose membranes. For  $\alpha$ -synuclein<sup>1-95</sup>, the following changes were introduced to avoid loss of the small protein from the nitrocellulose membrane, as described (*S25*): 1. Small pore-sized nitrocellulose membrane (0.2  $\mu$ m) was used; 2. Nitrocellulose membranes were completely dried after transfer; 3. Membranes were subjected to 15 min 0.2% glutaraldehyde in PBS to fix proteins on the membrane. Blots were blocked in Tris-buffered saline (TBS) containing 0.1% Tween-20 (Sigma) and 5% fat-free milk for 30 min at room temperature. The blocked membrane was incubated in blocking buffer containing primary antibody overnight at 4 °C, followed by 3-5 washes. The washed membrane was incubated in blocking buffer containing either horseradish peroxidase (HRP)-conjugated secondary antibody (MP biomedical, 1:8000) for 2 h at room temperature, or <sup>125</sup>I-labeled secondary antibody (Perkin Elmer, 1:1000) overnight at room temperature. HRP immunoblots were developed using enhanced chemiluminescence (GE healthcare). <sup>125</sup>I blots were exposed to a phosphorimager screen (Amersham) for 1-7 days and scanned using a Storm scanner (GE healthcare), followed by quantification with ImageQuant software (GE healthcare).

**Antibodies used.** *Monoclonal antibodies:*  $\beta$ -Actin (A1978, Sigma), CASK (cl. 7, BD Biosciences), GDI (cl. 81.2, SYSY), gephyrin (cl. 3B11, SYSY), GFAP (MAB360, Millipore), HA (cl. 16B12, Covance), Hsc70 (cl. 3C5, SYSY; 1B5, Affinity Bioreagents; SPA-815, Stressgen), LAMP-2 (H4B4, Santa Cruz), Munc-18 (cl. 31, BD Biosciences), c-Myc (9E10, Santa Cruz), NeuN (A60, Millipore), Neurofilament-H (2836, Cell Signaling), PSD-95 (MA1-046, Thermo Scientific), rab3 (cl. 42.4, SYSY), rabphilin-3A (cl. 47, BD Biosciences), SNAP-25 (SMI81, Sternberger Monoclonals; cl. 71.1, SYSY), synapsin (cl. 10.22, SYSY), synaptobrevin-2 (cl. 69.1, SYSY), synaptophysin (cl. 7.2, SYSY), syntaxin-1 (HPC1, SYSY),  $\alpha$ -synuclein (610786, BD-Transduction). *Polyclonal antibodies:* Caspase-3 cleaved (9661S, Cell Signaling), Complexin 1 and

2 (122 002, SYSY), CSP $\alpha$  (R807), Hsc70 (A903), NSF (P944), PSD-95 (L667), SCAMP-1 (P936), SGT (CHAT33),  $\alpha$ SNAP (J373), SNAP-23 (P914), SNAP-25 (P913), SV2 (P915), Synapsins (E028 and P586), synaptobrevin-2 (P939), synaptotagmin-1 (V216), syntaxin-1 (438B),  $\alpha$ -synuclein (T2270), VCP (K331), vGAT (131003, SYSY).

**Electrophysiology Recordings.** Acute hippocampal slices were prepared for extracellular recordings as described previously (S26). In brief, the brain was rapidly removed and immersed in ice cold dissection solution (in mM: 222 sucrose; 11 glucose; 26 NaHCO<sub>3</sub>; 1 NaH<sub>2</sub>PO<sub>4</sub>; 3 KCl; 7 MgCl<sub>2</sub>; 0.5 CaCl<sub>2</sub>). Slices were then made using a Leica VT 1200S. Following slicing, the slices were allowed to recover for 1 hour at room temperature in aCSF (in mM: 126 NaCl; 3 KCl; 1.25 NaH<sub>2</sub>PO<sub>4</sub>; 26 NaHCO<sub>3</sub>; 10 glucose; 2.5 CaCl<sub>2</sub>; and 1.3 MgCl<sub>2</sub> saturated with 95% O<sub>2</sub>/5% CO<sub>2</sub>, pH 7.4) prior to recording. All recordings were performed at 28-30°C. Extracellular field recordings were performed as follows: a patch pipette (2-3 M $\Omega$ ) filled with ACSF and a stimulating electrode were placed in the stratum radiatum of the CA1 region of the hippocampus. Input-output measurements were then conducted at various stimulus intensities by measuring the amplitude of the fiber-volley relative to the slope of the fEPSP. Paired-pulse facilitation (PPF) measurements were then performed by measuring the amplitude of fEPSP<sub>2</sub> relative to fEPSP<sub>1</sub> at various interstimulus intervals (50, 100, 200, 400, 600  $\mu$ s). Responses were set to 30-40% of the maximal response for PPF experiments. Traces were sampled at 0.1 Hz and minimum of 5-10 traces were averaged for each stimulus intensity or interstimulus interval. All recordings were digitized at 10 kHz and filtered at 1 kHz. Recordings were analyzed offline using pClamp. Statistical significance of data was evaluated using a Student's *t* test. All recordings were performed blind to genotype.

**Statistical analyses.** Unless stated otherwise, co-immunoprecipitation experiments are shown as recovered protein (relative to the input), which was first normalized to the immunoprecipitated protein and then normalized to the control (WT or control treatment). Prism software (GraphPad) was used to plot the survival and paralysis curves, followed by Log-rank (Mantel-Cox) and Gehan-Breslow-Wilcoxon (not shown) tests to assess statistical significance. Behavioral data were analyzed using StatView 5.0 software (SAS Institute), first by ANOVA, and in cases of significance ( $P < 0.05$ ), also by post hoc comparisons using Fisher's test. Prism software was used to analyze frequency distribution of NeuN:DAPI ratio from immunohistochemical data. All other data shown are means  $\pm$  SEMs, and were statistically analyzed by Student's unpaired two-tailed *t* test to compare the data groups. "n" refers to the number of different cultures or mice used in each group in separate experiments, or to the number of independent in vitro experiments.

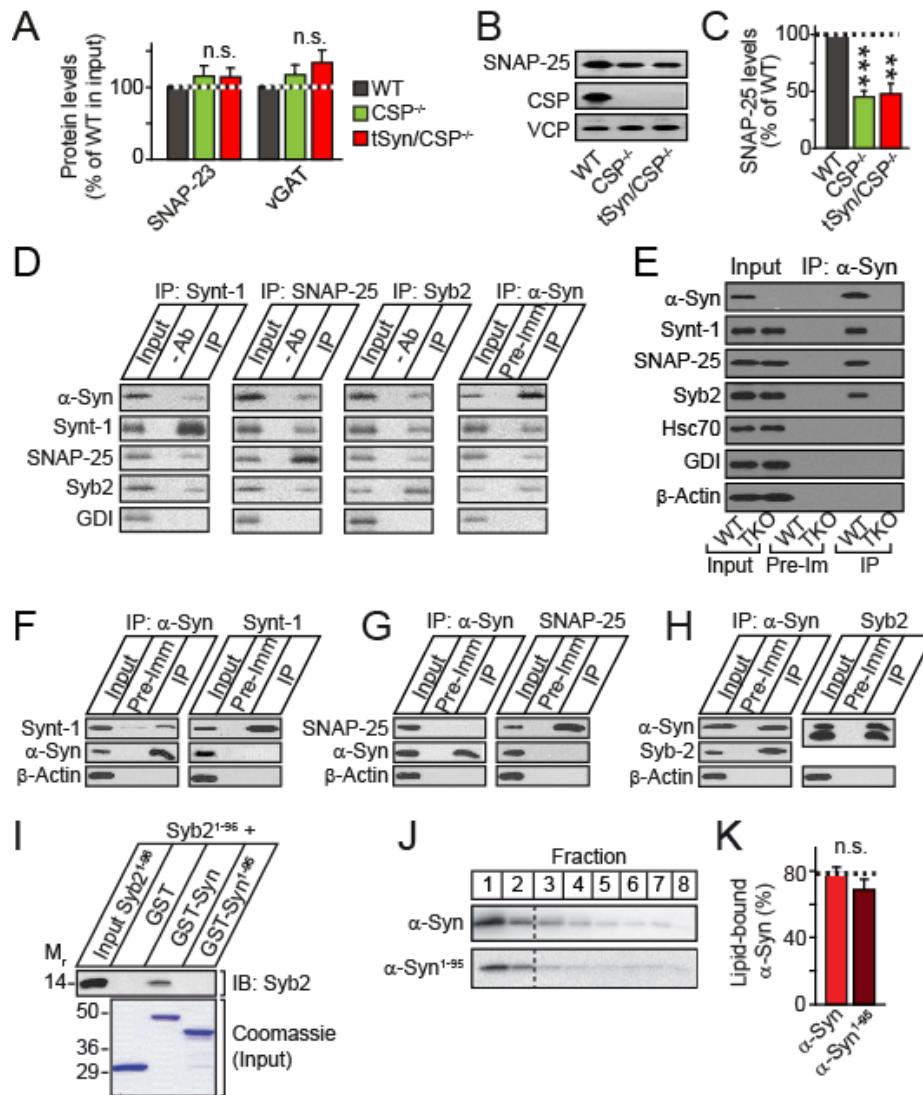


Figure S1

**α-Synuclein binding to synaptobrevin-2: effect of C-terminal truncation**

(A) Quantitations of total SNAP-23 and vGAT protein levels in mouse brains of indicated genotypes (additional data for Figs. 1A-1D).

(B & C) SNAP-25 levels are decreased in CSP $\alpha$  KO mice independent of transgenic  $\alpha$ -synuclein expression. Brain homogenates from WT and CSP $\alpha$  KO without or with expression of transgenic human  $\alpha$ -synuclein (tSyn) were analyzed by immunoblotting for SNAP-25, CSP $\alpha$  and VCP (B, representative blots; C, quantitations of SNAP-25 levels normalized to VCP).

(D)  $\alpha$ -Synuclein ( $\alpha$ -Syn) and neuronal SNARE complexes co-immunoprecipitate with each other from brain homogenates. SNARE complexes and  $\alpha$ -synuclein were immunoprecipitated from WT mouse brain lysates with antibodies to the individual SNARE proteins (Synt-1 = syntaxin-1; Syb2 = synaptobrevin-2) or  $\alpha$ -synuclein, respectively. Immunoprecipitates were analyzed by immunoblotting with the indicated antibodies; GDI was used as a specificity control (-Ab or Pre-Imm = control IPs either without primary antibody or using pre-immune serum).

(E)  $\alpha$ -Synuclein immunoprecipitations from WT and TKO brains. Performed as described in (D),  $\alpha$ -synuclein immunoprecipitations were analyzed for the indicated proteins by immunoblotting to



demonstrate that the same  $\alpha$ -synuclein antibody that brings down SNARE complexes in wild-type brains (D) does not bring down SNARE complexes in TKO brains lacking  $\alpha$ -synuclein.

**(F-H)** Syntaxin-1 and SNAP-25 do not directly bind to  $\alpha$ -synuclein, whereas synaptobrevin-2 does. HEK293T cells were separately co-transfected with expression vectors for  $\alpha$ -synuclein and syntaxin-1 (F), SNAP-25 (G), or synaptobrevin-2 (H), and cell lysates were immunoprecipitated either with antibodies to  $\alpha$ -synuclein (left panels), or to syntaxin-1, SNAP-25 or synaptobrevin-2 (right panels), using pre-immune sera (Pre-Imm) as a control. Immunoprecipitates were analyzed by immunoblotting, with  $\beta$ -actin as a negative control.

**(I)** GST-fusion proteins of full-length but not C-terminally truncated  $\alpha$ -synuclein pull down recombinant synaptobrevin-2 lacking a transmembrane region (Syb2<sup>1-96</sup>). Immobilized GST, GST-Syn or GST-Syn<sup>1-95</sup> fusion proteins (see Coomassie for input) were incubated with purified Syb2<sup>1-96</sup>. Bound proteins were analyzed by immunoblotting for synaptobrevin-2.

**(J & K)** Full-length  $\alpha$ -synuclein ( $\alpha$ -Syn) and C-terminally truncated  $\alpha$ -synuclein ( $\alpha$ -Syn<sup>1-95</sup>) equally bind to liposomes. Purified full-length or C-terminally truncated  $\alpha$ -synuclein were incubated with liposomes and subjected to a flotation assay in a density gradient (for principle, see Fig. 2G). Equal volumes of each fraction were analyzed by immunoblotting (J), and bound protein in fractions 1 and 2 was quantified as fraction of total protein (K).

Protein measurements were performed by quantitative immunoblotting; data are means  $\pm$  SEMs, \* =  $p < 0.05$ ; \*\* =  $p < 0.01$ ; \*\*\* =  $p < 0.001$  (n = 3-5).

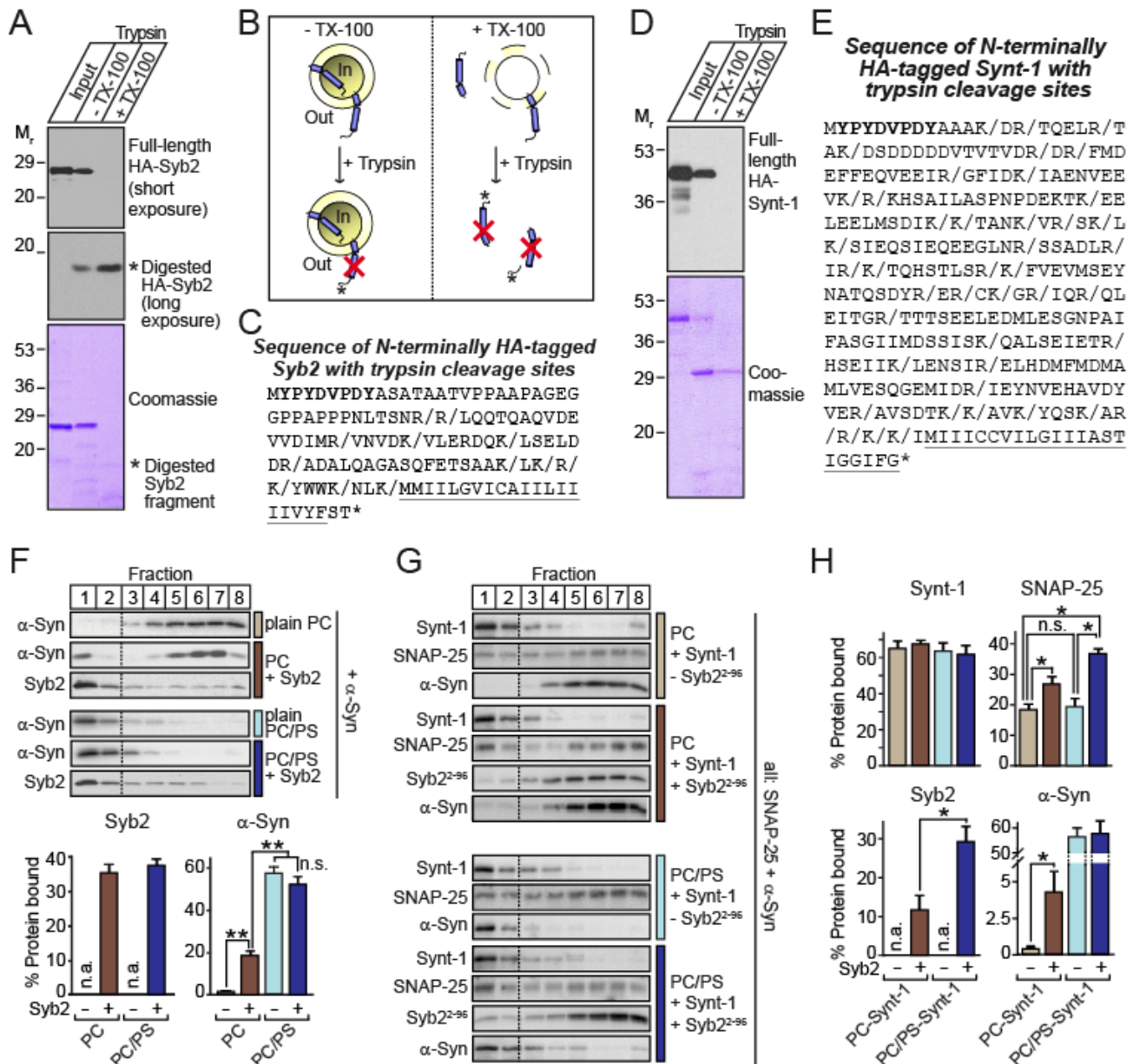


**Figure S2**

**SNARE protein reconstitution into liposomes: synaptobrevin-2 mediates binding of  $\alpha$ -synuclein to neutral liposomes**

(A) Analysis of synaptobrevin-2 membrane topology after liposome reconstitution. Liposomes containing reconstituted HA-tagged synaptobrevin-2 (HA-Syb2) were incubated with trypsin with or without 0.2% Triton X-100 (TX-100). Samples were analyzed by immunoblotting for Syb2 (lower of the top two panels exhibits long exposure to visualize the small N-terminal tryptic fragment that is only poorly retained on the blotting membrane), or by Coomassie-blue staining (bottom panel). Note that in the absence of TX-100, ~50% of synaptobrevin-2 is protected from proteolysis, and that a trypsin-resistant small fragment can be detected after long exposure, which increases in the presence of TX-100 (asterisk = small trypsin-resistant fragment detected by HA antibody).

(B) Schematic diagram of the trypsin digestion experiment of panel A.

(C) Sequence of HA-Syb2 with indicated tryptic cleavage sites (slashes), HA-epitope tag (**bold**) and the transmembrane region (underlined). Note that the largest tryptic fragment is the N-terminal sequence containing the HA epitope tag.

(D & E) Analysis of the membrane topology of syntaxin-1 reconstituted into liposomes and digested with trypsin without or with Triton X-100 as described in (A), and sequence of HA-Synt-1 with trypsin cleavage sites as described in (C).

(F)  $\alpha$ -Synuclein binds to neutral liposomes only when these liposomes contain synaptobrevin-2. Neutral (PC) or charged (PC/PS) liposomes containing or lacking reconstituted full-length synaptobrevin-2 (Syb2) were mixed with recombinant  $\alpha$ -synuclein and subjected to a flotation assay as described (see Fig. 2G). Representative immunoblots of  $\alpha$ -synuclein and synaptobrevin-2 (top panel) and quantitations of protein (bottom panel) in the top two (liposome-bound) fractions are shown. Note that consistent with previous studies (S27),  $\alpha$ -synuclein binds to liposomes directly only when these liposomes contain negatively charged phospholipids, but that reconstituted synaptobrevin-2 in neutral liposomes confers binding of  $\alpha$ -synuclein to these liposomes.

(G & H)  $\alpha$ -Synuclein does not bind to neutral liposomes containing syntaxin-1 or SNAP-25. PC or PC/PS liposomes containing reconstituted full-length HA-Synt-1 were mixed with SNAP-25 and  $\alpha$ -synuclein, with or without soluble Syb2<sup>1-96</sup>, and samples were subjected to a flotation assay to identify proteins bound to the liposomes (G, representative blots; H, quantitations of protein to floated liposomes). Note, that  $\alpha$ -synuclein does not float up with the liposomes in presence of neutral liposomes containing syntaxin-1 and SNAP-25; but that addition of soluble synaptobrevin-2 confers  $\alpha$ -synuclein binding.

Protein measurements were performed by quantitative immunoblotting, and are shown as means  $\pm$  SEMs, \* =  $p < 0.05$ ; \*\* =  $p < 0.01$  (n = 5-10).

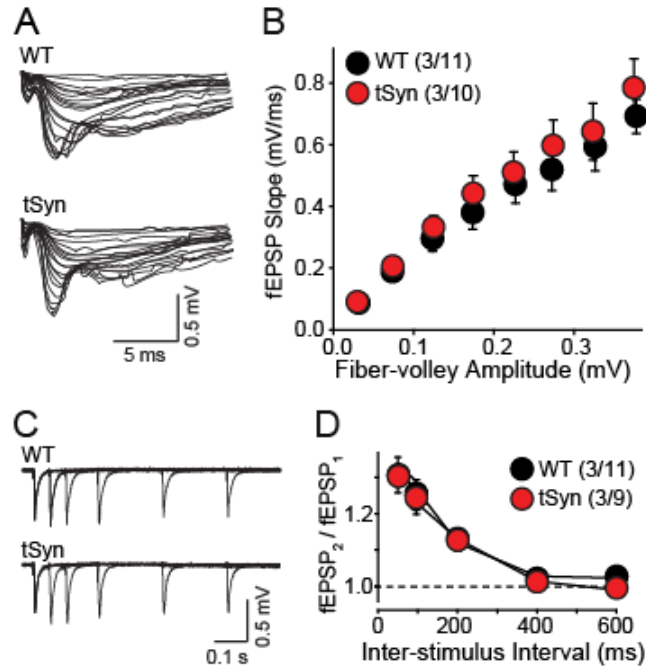


**Figure S3**

(A & B) Transgenic  $\alpha$ -synuclein does not inhibit synaptic transmission. Sample traces (A) and summary graphs (B) from extracellular field recordings of excitatory post-synaptic potentials (fEPSPs) in acute hippocampal slices from littermate WT (3 mice, 11 slices) or transgenic  $\alpha$ -synuclein mice (tSyn; 3 mice, 10 slices). The fEPSP slope is plotted as a function of the fiber volley amplitude at increasing stimulus intensities.

(C & D) Normal short-term plasticity in  $\alpha$ -synuclein transgenic mice suggests a normal release probability. Data show sample traces (C) and a summary graph (D) of the ratio of fEPSP slopes induced by two closely spaced stimuli applied with increasing inter-stimulus intervals (WT, 3 mice, 11 slices; tSyn, 3 mice, 9 slices). All recordings were done in the stratum radiatum of the CA1 region of the hippocampus. Graphs represent means  $\pm$  SEM; there is no statistically significant difference between wild-type and transgenic  $\alpha$ -synuclein samples.

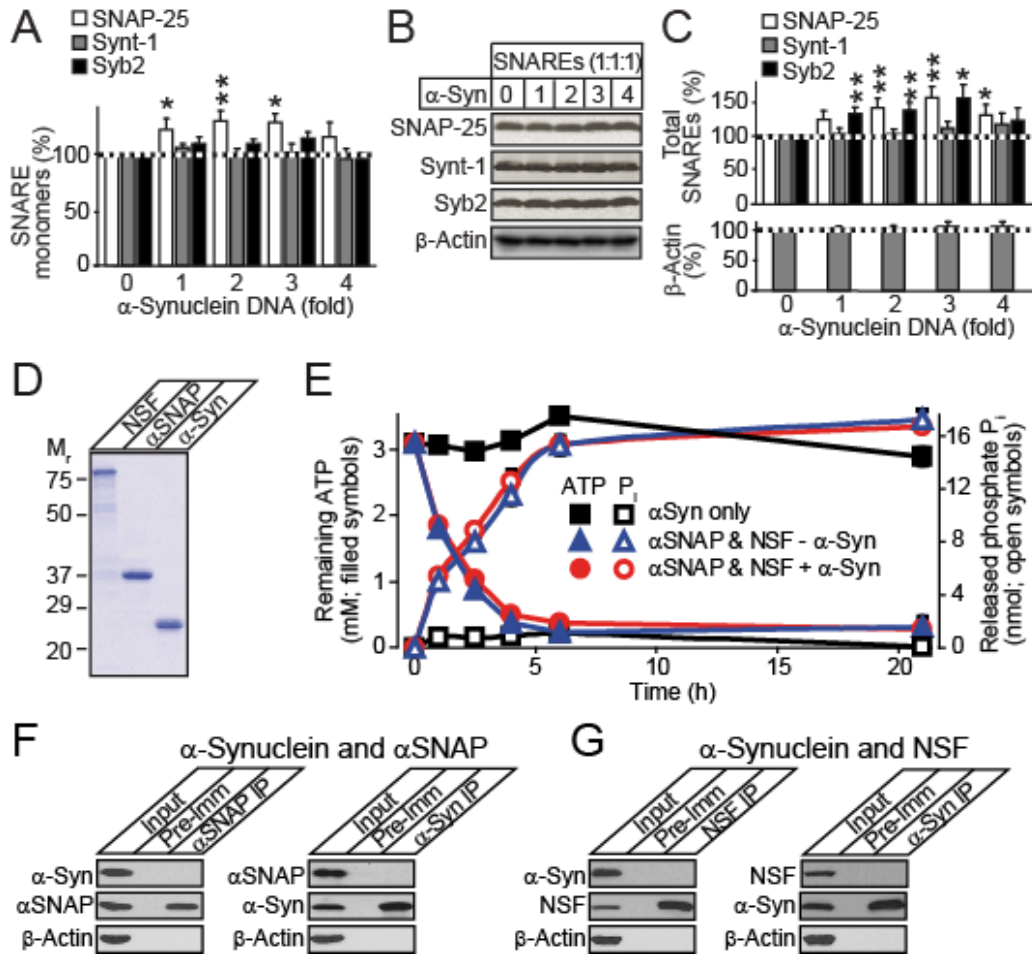


Figure S4

**Effect of  $\alpha$ -synuclein on transfected SNARE protein levels and NSF ATPase activity, and lack of  $\alpha$ -synuclein binding to NSF and  $\alpha$ SNAP**

(A) HEK293T cells were co-transfected with plasmids expressing syntaxin-1 (Synt-1), synaptobrevin-2 (Syb2), and SNAP-25 in a 1:1:1 ratio, together with an increasing amount of  $\alpha$ -synuclein ( $\alpha$ -Syn) expression plasmid. Cell lysates were immunoblotted for the indicated SNAREs, followed by quantitation (for representative immunoblots, see Fig. 2A, right panel).

(B & C) Total expression of individual SNARE proteins in transfected HEK293 cells was analyzed by melting SNARE-complexes in SDS sample buffer (100 °C for 20 min), and quantitated by immunoblotting, normalized to  $\beta$ -actin levels (B, representative blots; C, quantitations).

(D) Coomassie-stained SDS gel of purified NSF,  $\alpha$ SNAP, and  $\alpha$ -synuclein recombinant proteins.

(E) Effect of  $\alpha$ -synuclein on NSF ATPase activity. The ATPase activity of  $\alpha$ SNAP and NSF with or without  $\alpha$ -synuclein was determined using quantitation of remaining ATP (Kinase-Glo assay; left y-axis) or of released inorganic phosphate P<sub>i</sub> (Lanzetta assay; right y-axis) at the indicated time points.

(F & G)  $\alpha$ -Synuclein does not directly interact with  $\alpha$ SNAP or NSF. Lysates from HEK293T cells transfected with equimolar amounts of DNA for  $\alpha$ -synuclein and  $\alpha$ SNAP (F) or  $\alpha$ -synuclein and NSF (G) were immunoprecipitated with antibodies against  $\alpha$ -synuclein or  $\alpha$ SNAP (F), or  $\alpha$ -synuclein or NSF (G). Immunoprecipitated proteins were detected by immunoblotting as indicated.

Protein measurements were performed by quantitative immunoblotting. Data shown are means  $\pm$  SEMs, \* = p<0.05; \*\* = p<0.01 (n = 3-9).

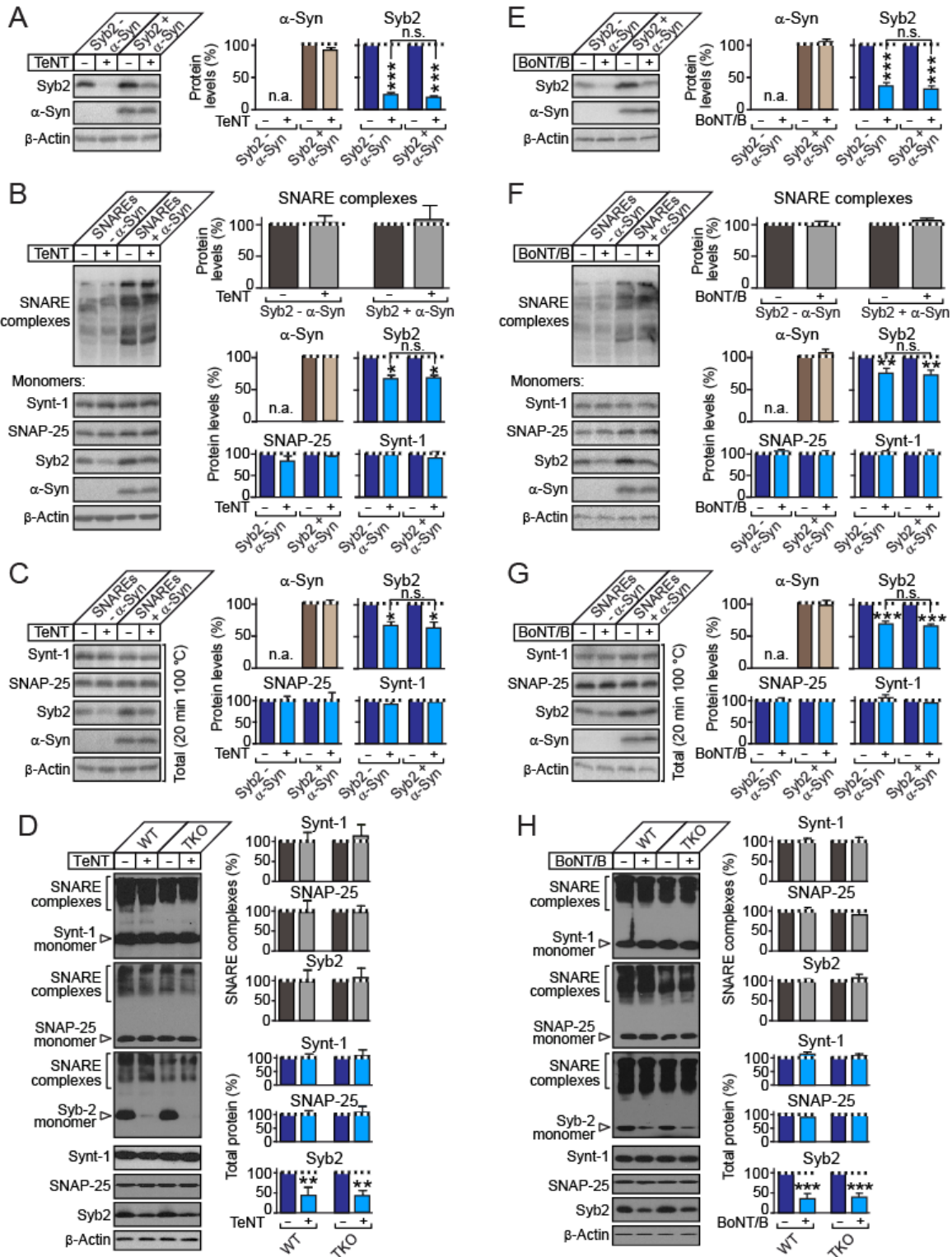


Figure S5

**$\alpha$ -Synuclein does not alter the resistance of SNARE complexes to cleavage by tetanus or botulinum toxin.**

(A) Synaptobrevin-2 is cleaved by tetanus toxin light chain (TeNT) in transfected HEK293 cells. Synaptobrevin-2 (Syb2) was transfected with or without 4-fold amounts of  $\alpha$ -synuclein ( $\alpha$ -Syn) expression vector, and cell lysates were mixed with a lysate from tetanus toxin (TeNT)-transfected

or untransfected HEK cells. Protein levels were analyzed by quantitative immunoblotting (representative immunoblots: left panels; quantitations: right panels), normalized to  $\beta$ -actin levels.

**(B & C)** All three SNARE proteins were transfected with or without  $\alpha$ -synuclein and mixed with TeNT-transfected HEK lysates. SNARE complex levels and monomeric SNARE protein levels (B), as well as total SNARE levels (C) were analyzed by quantitative immunoblotting (Synt-1 = syntaxin-1).

**(D)** TeNT does not change SNARE complex levels in WT and TKO brain lysates, but cleaves synaptobrevin-2. Brain lysates from WT and TKO mice were mixed with lysates from TeNT-transfected or untransfected HEK cells. SNARE complex levels and total SNARE proteins levels were analyzed by quantitative immunoblotting.

**(E-H)** Experiments analogous to those described for panels A-D, but using transfected botulinum toxin B light chain (BoNT/B) instead of tetanus toxin light chain.

Protein measurements were performed by quantitative immunoblotting, and are shown as means  $\pm$  SEMs, \* =  $p < 0.05$ ; \*\* =  $p < 0.01$ ; \*\*\* =  $p < 0.001$  (n = 3-5).



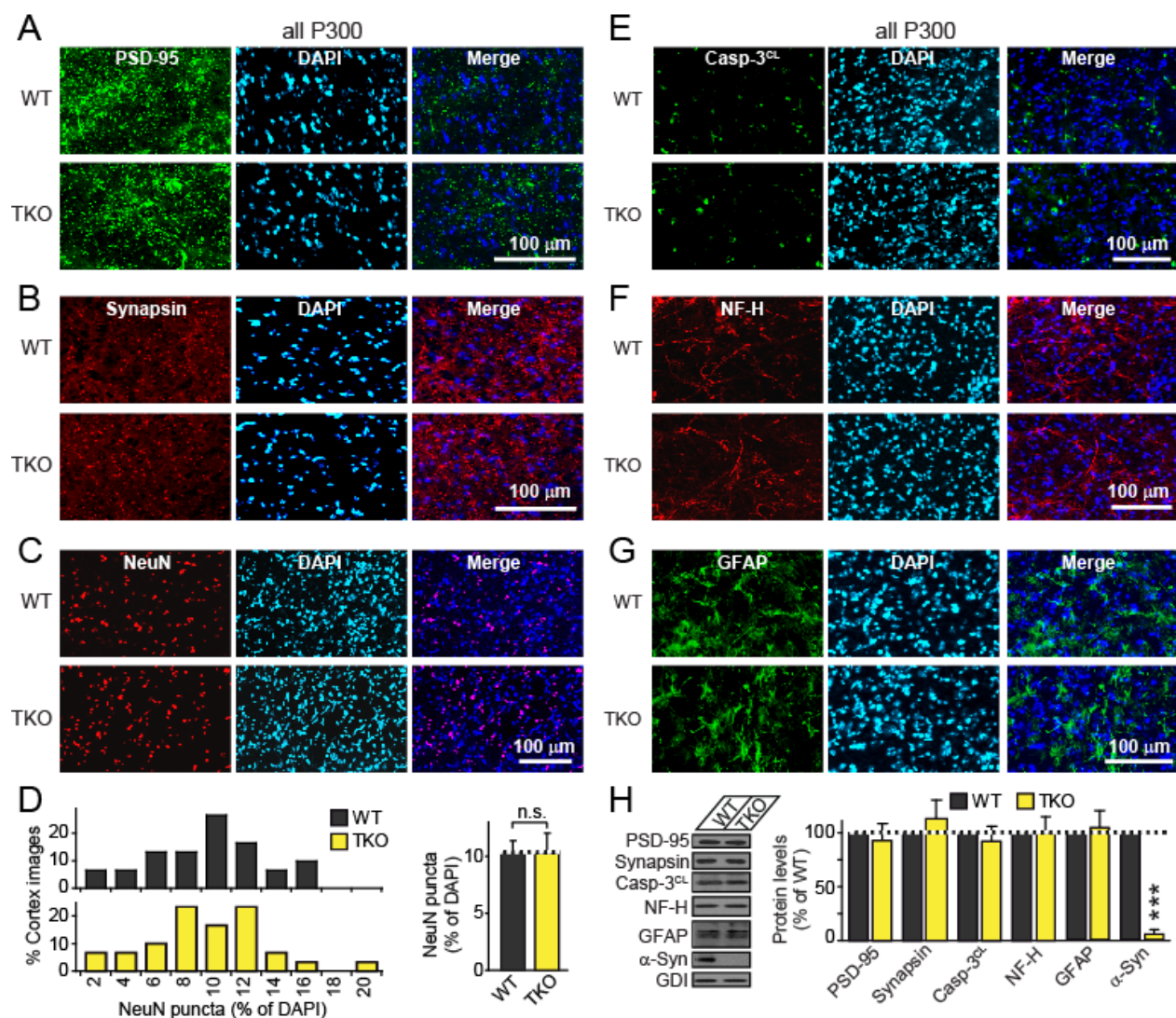


**Figure S6**

**Synaptic and neuronal density and gliosis studies in TKO brains**

(A-G) Sections from brains of aged WT and TKO mice (at P300) were immunostained for markers of synaptic and neuronal density, and for markers of apoptosis and gliosis. (A & B) PSD-95 and synapsin were stained as post- and pre-synaptic markers of synapse density. (C) Neurons were stained with NeuN antibody and all nuclei were counterstained with DAPI to calculate neuron density as a fraction of total cellular density. (D) Neuronal density was measured by counting NeuN-positive puncta as percent of DAPI puncta (n = 30 images from 3 brains of each, WT and TKO). (E-G) Markers of neurodegeneration were visualized by immunostaining for cleaved caspase-3 (Casp-3<sup>CL</sup>; E), neurofilament heavy-chain (NF-H; F), and glial fibrillary acidic protein (GFAP; G).

(H) Markers of synaptic density, neuronal density and neurodegeneration shown above were measured by immunoblotting brain lysates of aged WT and TKO mice (at P300). Protein levels were measured by quantitative immunoblotting and normalized to GDI (n = 3; data are means ± SEMs, \* = p<0.05; \*\* = p<0.01; \*\*\* = p<0.001).



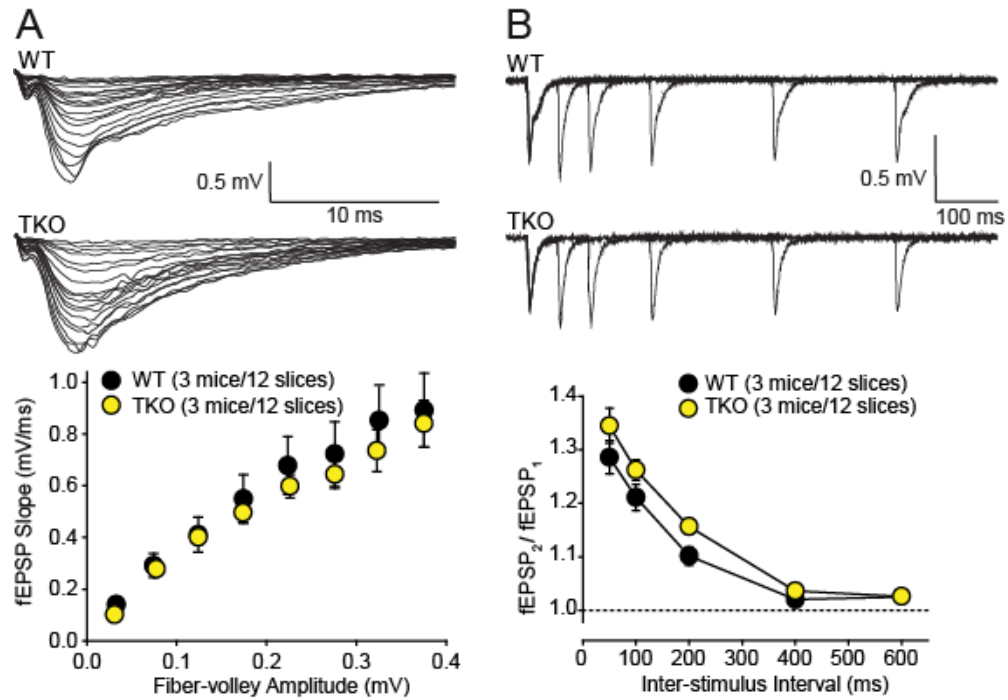
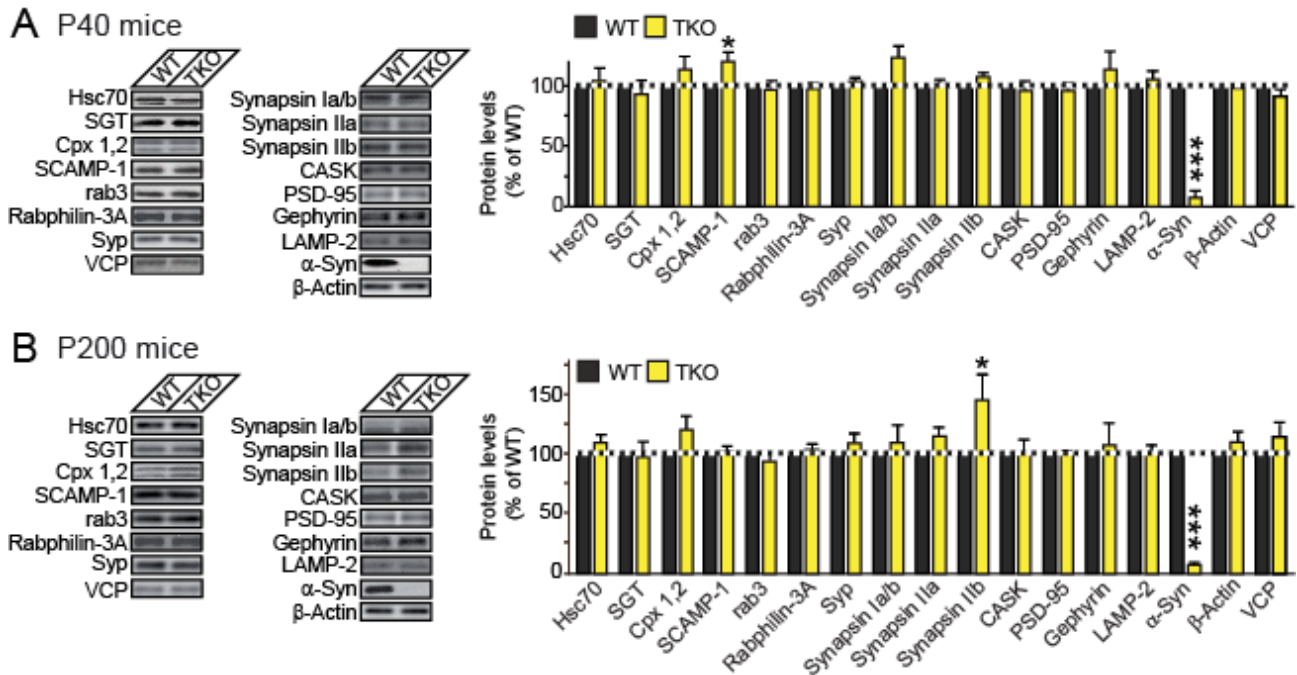


Figure S7

### Synaptic function in TKO mice

Deletion of  $\alpha\beta\gamma$ -synuclein does not impair excitatory synaptic transmission. (A) Sample traces and summary graph for input-output fEPSP measurements in WT (3 mice, 12 slices) and  $\alpha\beta\gamma$ -synuclein triple knockout (TKO) mice (3 mice, 12 slices). Extracellular recordings were performed in the stratum radiatum of the CA1 region of acute hippocampal slices. (B) Sample traces and summary graph for paired-pulse facilitation experiments, recorded at various inter-stimulus intervals in wild-type (3 mice, 12 slices) and  $\alpha\beta\gamma$ -synuclein KO (3 mice, 12 slices) mice. Data represents mean  $\pm$  SEM.



**Figure S8**

**Age-dependent changes in synaptobrevin-2 and CSP $\alpha$  levels in  $\alpha\beta\gamma$ -synuclein TKO mice**

(A & B) Effect of  $\alpha\beta\gamma$ -synuclein TKO on neuronal protein levels in young (P40, A) and aged mice (P200, B). Neuronal protein levels (left panels, representative immunoblots; right panels, summary graphs) were measured in brain lysates from WT and TKO mice at P40 and P200 by quantitative immunoblotting. See Figure 3E for additional proteins, and abbreviations table for full names of the proteins analyzed.

All protein levels were measured by quantitative immunoblotting (n = 3-8; data are means  $\pm$  SEMs, \* = p<0.05; \*\* = p<0.01; \*\*\* = p<0.001).

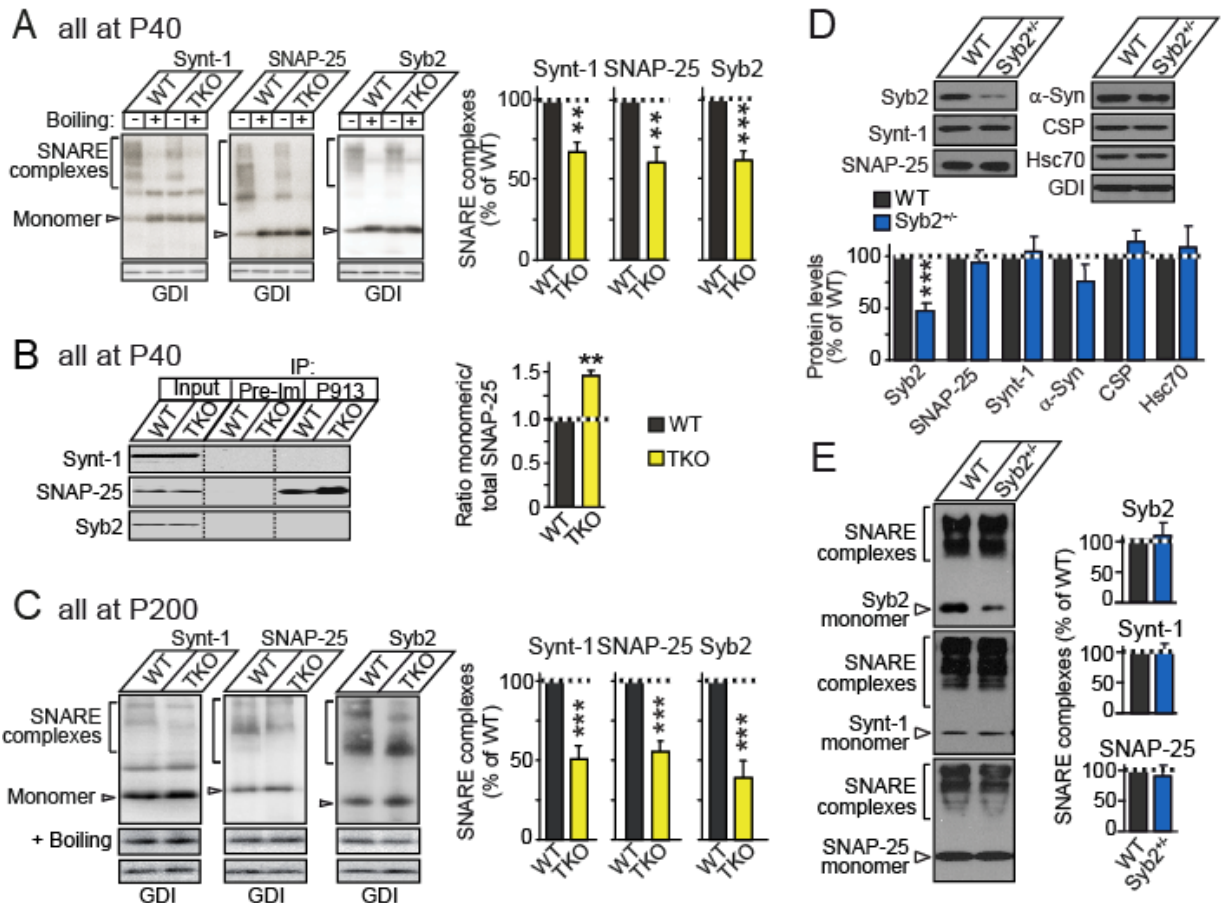


Figure S9

**SNARE-complex assembly is reduced in brain homogenates from  $\alpha\beta\gamma$ -synuclein TKO mice**

(A & B) Analysis of SNARE-complex levels in WT and TKO mouse brains at P40. In (A), SNARE-complex levels were measured by SDS-PAGE of non-boiled samples, with quantification of high-molecular mass bands reacting with SNARE protein antibodies (left = representative blots; right = summary graph of quantitations obtained in multiple independent experiments); note that the high-molecular mass bands are abolished by boiling. In (B), SNARE-complex levels are measured by immunoprecipitation of SNAP-25 with an antibody (P913) that recognizes only monomeric SNAP-25 (left = representative blots; Pre-Im, preimmune serum); the ratio of monomeric to total levels is calculated, which is inversely proportional to SNARE-complex levels (right).

(C) Analysis of SNARE-complex assembly in WT and TKO mouse brains similar to panel (A), except that the experiments were carried out with brains harvested at P200, and that boiled and non-boiled samples are not run side-by-side, but separately as indicated (left = representative blots; right = quantitations). Note that the relative extent of the SNARE-complex assembly deficit in TKO mice analyzed with this method, and the age-dependent increase in the deficit, are similar to that observed with the co-immunoprecipitation method as shown in Fig. 3F.

(D & E) Expression levels of indicated proteins and SNARE complex assembly were quantitated from brain lysates of WT and Syb2 heterozygous (Syb2<sup>+/-</sup>) mice (at P40). (D) Synaptobrevin expression is reduced by ~50% in Syb2<sup>+/-</sup> brains. All proteins levels were normalized to loading control GDI. (E) SNARE complexes were measured by immunoblotting with Syb2, Synt-1 and SNAP-25 antibodies as high molecular mass bands from non-boiled samples.

All protein levels were measured by quantitative immunoblotting using <sup>125</sup>I-labeled secondary antibodies (n = 3-8; data are means ± SEMs, \* = p<0.05; \*\* = p<0.01; \*\*\* = p<0.001).

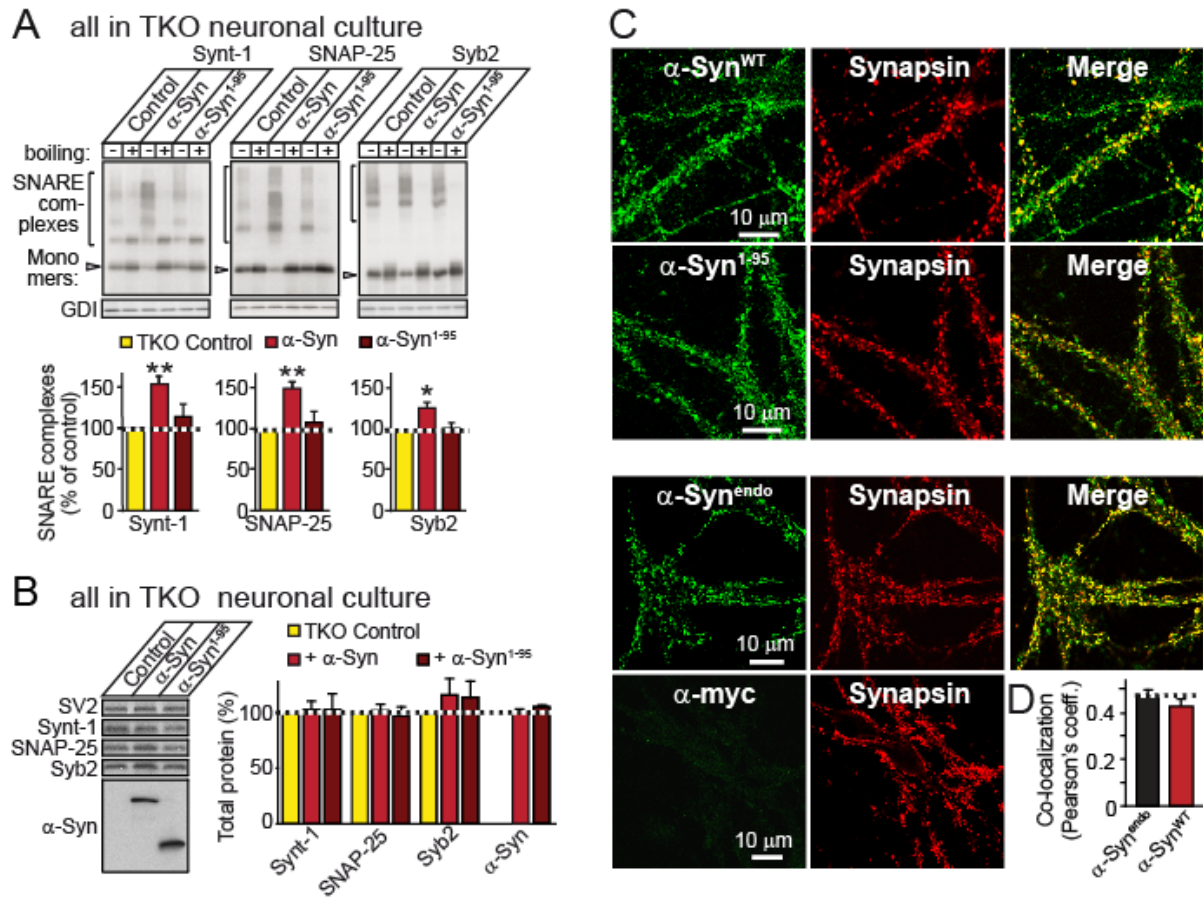


Figure S10

**$\alpha$ -Synuclein but not  $\alpha$ -synuclein<sup>1-95</sup> promotes SNARE-complex assembly in TKO neurons, although both are targeted to synapses**

(A) Selective rescue of the SNARE-complex assembly deficit in TKO neurons by full-length ( $\alpha$ -Syn) but not C-terminally truncated human  $\alpha$ -synuclein ( $\alpha$ -Syn<sup>1-95</sup>). TKO neurons were infected with lentiviruses expressing myc- $\alpha$ -Syn, myc- $\alpha$ -Syn<sup>1-95</sup>, or plain virus (control), and SNARE-complex assembly was analyzed by immunoblotting non-boiled samples. Representative blots are shown on top, and quantitations of SNARE complex levels on the bottom.

(B) Effect of  $\alpha$ -Syn and  $\alpha$ -Syn<sup>1-95</sup> on total SNARE protein levels in TKO neuronal cultures was assessed by immunoblotting for SV2, syntaxin-1 (Synt-1), SNAP-25, synaptobrevin-2 (Syb2), and  $\alpha$ -Syn (left panels), followed by quantitation and normalization to SV2 levels (right panels).

Protein levels in (A) and (B) were measured by quantitative immunoblotting. Data shown are means  $\pm$  SEMs, \* =  $p < 0.05$ ; \*\* =  $p < 0.01$  (n = 3-5).

(C & D) Synaptic targeting of full-length and C-terminally truncated  $\alpha$ -synuclein. Cultured hippocampal rat neurons were infected with lentiviruses expressing myc-tagged full-length ( $\alpha$ -Syn) or truncated  $\alpha$ -synuclein ( $\alpha$ -Syn<sup>1-95</sup>) at DIV7, and analyzed by immunofluorescence at DIV19 (myc = green; synapsin = red). Uninfected neurons were stained for endogenous  $\alpha$ -synuclein ( $\alpha$ -Syn<sup>endo</sup>; top panels), and for background anti-myc staining (bottom panels). Synaptic targeting of endogenous and exogenous  $\alpha$ -synuclein was quantified using Pearson's coefficient (D).

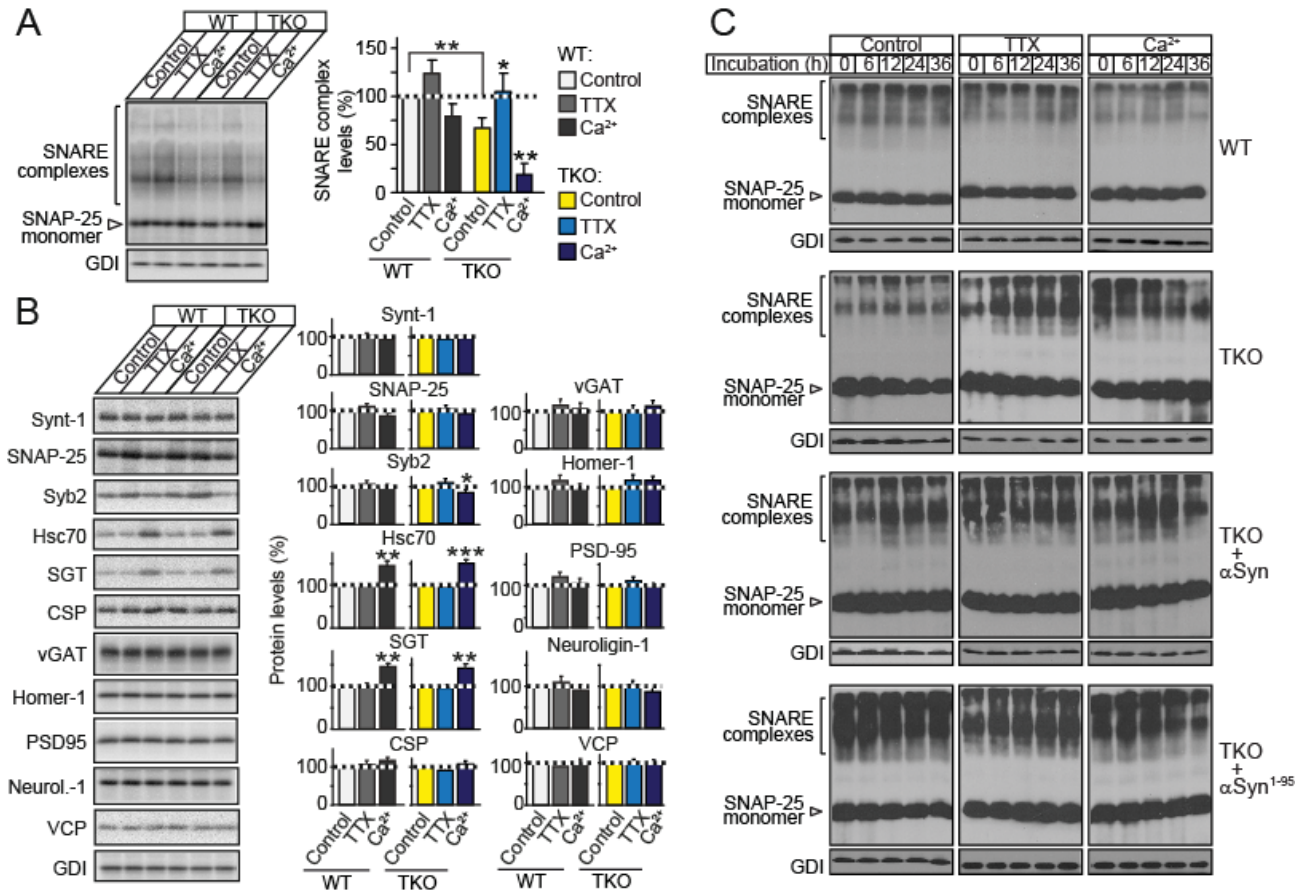


**Figure S11**

**Effect of synaptic activity on synuclein-dependent SNARE-complex assembly**

(A) Activity-dependence of the deficit in SNARE-complex assembly induced by the  $\alpha\beta\gamma$ -synuclein TKO. Cortical neurons cultured from WT and TKO mice were incubated at DIV10 for 36 hrs in control medium or medium containing 0.5  $\mu$ M TTX or 4 mM Ca<sup>2+</sup>. SNARE complexes were measured as high-molecular mass immunoreactive bands using non-boiled samples (for co-immunoprecipitation assays, see Fig. 4C).

(B) Quantitations of total protein levels in cultured WT and TKO neurons incubated in control medium or medium inhibiting (TTX) or promoting synaptic activity (Ca<sup>2+</sup>). For SNARE-complex assembly measurements using co-immunoprecipitation assays in the same samples, see Fig. 4C).

(C) Representative blots for the data shown in Fig. 4D, measuring the time course of the effect of synaptic silencing or stimulation on SNARE-complex assembly. Neuronal cultures from WT and TKO mice, and TKO cultures expressing either full-length ( $\alpha$ -Syn) or C-terminally truncated  $\alpha$ -synuclein ( $\alpha$ -Syn<sup>1-95</sup>) were incubated in control medium, in 0.5  $\mu$ M tetrodotoxin (TTX), or in 4 mM Ca<sup>2+</sup> (Ca<sup>2+</sup>) for the indicated times. SNARE-complex assembly was measured by immunoblotting for SNAP-25 and quantitating high-molecular mass SNARE complexes.

All protein levels were measured by quantitative immunoblotting (n = 3-6; data are means  $\pm$  SEMs, \* = p<0.05; \*\* = p<0.01; \*\*\* = p<0.001 by Student's t-test).



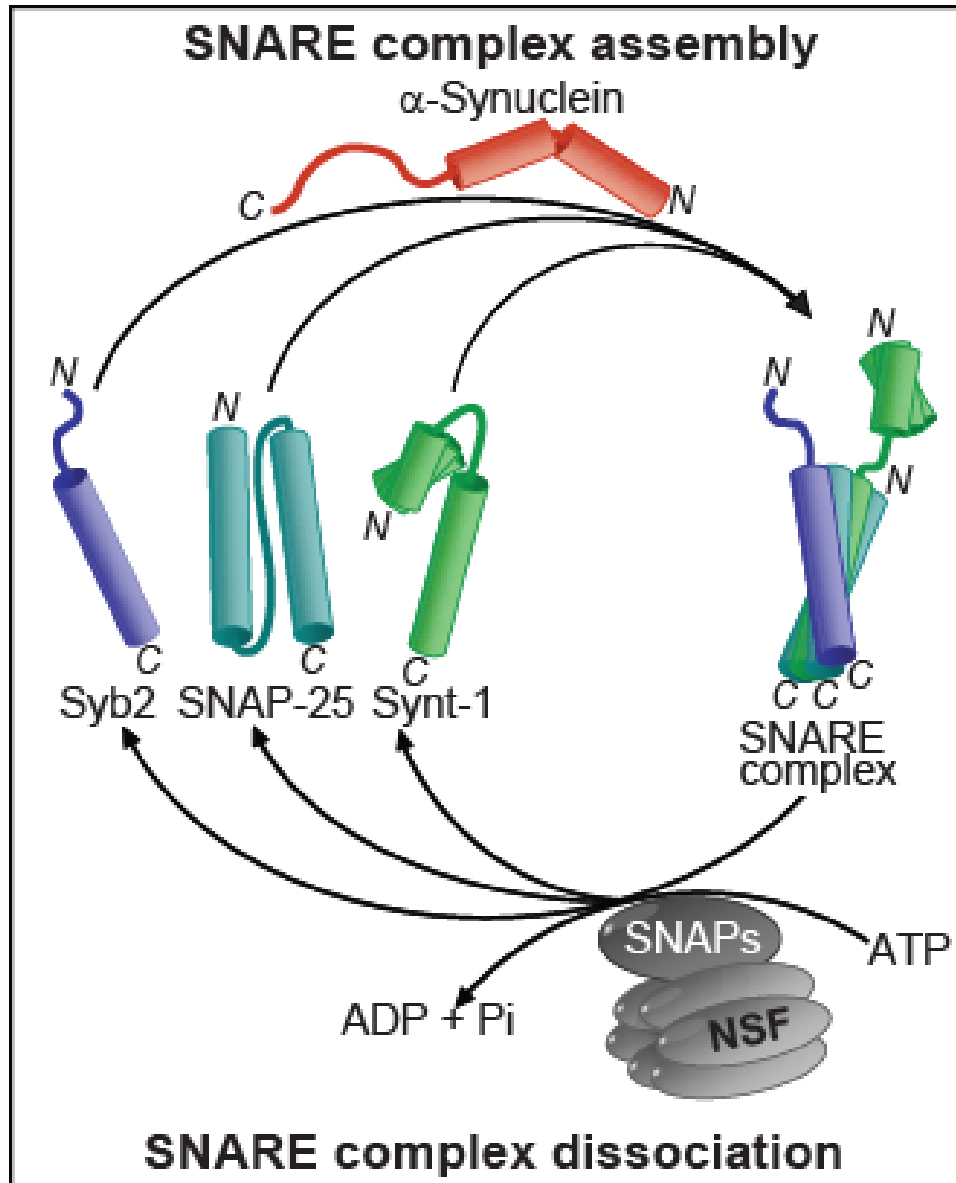


Figure S12

**Model depicting the promotion of SNARE-complex assembly by  $\alpha$ -synuclein during the SNARE cycle**

The model proposes that  $\alpha$ -synuclein promotes SNARE-complex assembly via direct interaction with synaptobrevin-2 (Syb2).  $\alpha$ -Synuclein acts by a non-classical chaperone activity that is ATP-independent, but involves  $\alpha$ -synuclein binding to phospholipids simultaneously with SNARE-binding. Assembled SNARE complexes are subsequently dissociated by a classical chaperone-complex composed of N-ethylmaleimide-sensitive factor (NSF) and SNAPs. Synaptobrevin-2 (Syb2) and syntaxin-1 (Synt-1) are depicted without their C-terminal transmembrane regions; N- and C-termini of SNARE proteins and  $\alpha$ -synuclein are indicated.

## SUPPLEMENTARY REFERENCES

- S1. R. Fernandez-Chacon *et al.*, The synaptic vesicle protein CSP $\alpha$  prevents presynaptic degeneration. *Neuron* **42**, 237-251 (2004).
- S2. S. Chandra, G. Gallardo, R. Fernandez-Chacon, O. M. Schlüter, T. C. Südhof,  $\alpha$ -Synuclein cooperates with CSP $\alpha$  in preventing neurodegeneration. *Cell* **123**, 383-396 (2005).
- S3. S. Chandra *et al.*, Double-knockout mice for  $\alpha$ - and  $\gamma$ -synucleins: effect on synaptic functions. *Proc Natl Acad Sci U S A* **101**, 14966-14971 (2004).
- S4. N. Ninkina *et al.*, Neurons expressing the highest levels of  $\gamma$ -synuclein are unaffected by targeted inactivation of the gene. *Mol Cell Biol* **23**, 8233-8245 (2003).
- S5. R. J. Carter, Characterization of progressive motor deficits in mice transgenic for the human Huntington's disease mutation. *J Neurosci* **19**, 3248-3257 (1999).
- S6. G. Gallardo, O. M. Schlüter, T. C. Südhof, A molecular pathway of neurodegeneration linking alpha-synuclein to ApoE and Abeta peptides. *Nat Neurosci* **11**, 301-308 (2008).
- S7. R. W. Burgess, G. A. Cox, K. L. Seburn, Neuromuscular disease models and analysis. *Methods Mol Biol* **602**, 347-393 (2010).
- S8. J. N. Crawley, Behavioral phenotyping of transgenic and knockout mice: experimental design and evaluation of general health, sensory functions, motor abilities, and specific behavioral tests. *Brain Res* **835**, 18-26 (1999).
- S9. T. Karl, R. Pabst, S. von Hörsten, Behavioral phenotyping of mice in pharmacological and toxicological research. *Exp Toxicol Pathol* **55**, 69-83 (2003).
- S10. A. Maximov, Z. P. Pang, D. G. Tervo, T. C. Südhof, Monitoring synaptic transmission in primary neuronal cultures using local extracellular stimulation. *J Neurosci Methods* **161**, 75-87 (2007).
- S11. J. Tang *et al.*, A complexin/synaptotagmin 1 switch controls fast synaptic vesicle exocytosis. *Cell* **126**, 1175-1187 (2006).
- S12. P. Salmon, D. Trono, Production and titration of lentiviral vectors. *Curr Protoc Neurosci Chapter 4* (2006).
- S13. C. Lois, E. J. Hong, S. Pease, E. J. Brown, D. Baltimore, Germline transmission and tissue-specific expression of transgenes delivered by lentiviral vectors. *Science* **295**, 868-872 (2002).
- S14. A. Ho, X. Liu, T. C. Südhof, Deletion of Mint proteins decreases amyloid production in transgenic mouse models of Alzheimer's disease. *J Neurosci* **28**, 14392-14400 (2008).
- S15. J. Aoto, C. I. Nam, M. M. Poon, P. Ting, L. Chen, Synaptic signaling by all-trans retinoic acid in homeostatic synaptic plasticity. *Neuron* **60**, 308-320 (2008).
- S16. K. Mukherjee *et al.*, CASK Functions as a Mg<sup>2+</sup>-independent neurexin kinase. *Cell* **133**, 328-339 (2008).
- S17. T. Hayashi *et al.*, Synaptic vesicle membrane fusion complex: action of clostridial neurotoxins on assembly. *EMBO J* **13**, 5051-5061 (1994).
- S18. S. Sugita, T. C. Südhof, Specificity of Ca<sup>2+</sup>-dependent protein interactions mediated by the C2A domains of synaptotagmins. *Biochemistry* **39**, 2940-2949 (2000).
- S19. L. P. Haynes, R. J. O. Barnard, A. Morgan, R. D. Burgoyne, Stimulation of NSF ATPase activity during t-SNARE priming. *FEBS Letters* **436**, 1-5 (1998).
- S20. P. A. Lanzetta, L. J. Alvarez, P. S. Reinach, O. A. Candia, An improved assay for nanomol amounts of inorganic phosphate. *Anal Biochem* **100**, 95-97 (1979).
- S21. Y. Barenholz *et al.*, A simple method for the preparation of homogeneous phospholipid vesicles. *Biochemistry* **16**, 2806-2810 (1977).

- S22. X. Chen *et al.*, SNARE-mediated lipid mixing depends on the physical state of the vesicles. *Biophys J* **90**, 2062-2074 (2006).
- S23. W. C. Tucker, T. Weber, E. R. Chapman, Reconstitution of Ca<sup>2+</sup>-regulated membrane fusion by synaptotagmin and SNAREs. *Science* **304**, 435-438 (2004).
- S24. T. W. Rosahl *et al.*, Essential functions of synapsins I and II in synaptic vesicle regulation. *Nature* **375**, 488-493 (1995).
- S25. B. T. Kurien, R. H. Scofield, A brief review of other notable protein detection methods on blots. *Methods Mol Biol* **536**, 557-571 (2009).
- S26. M. R. Etherton, C. A. Blaiss, C. M. Powell, T. C. Sudhof, Mouse neurexin-1 $\alpha$  deletion causes correlated electrophysiological and behavioral changes consistent with cognitive impairments. *Proc Nat Acad Sci U S A*. **106**, 17998-18003 (2009).
- S27. W. S. Davidson, A. Jonas, D. F. Clayton, J. M. George, Stabilization of alpha-synuclein secondary structure upon binding to synthetic membranes. *J. Biol. Chem.* **273**, 9443-9449 (1998).